Growth of Pore Interfaces and Roughness of Fracture Surfaces in Porous Silica: Million Particle Molecular-Dynamics Simulations

Aiichiro Nakano, Rajiv K. Kalia, and Priya Vashishta

Concurrent Computing Laboratory for Materials Simulations, Department of Physics and Astronomy, Department of Computer Science, Louisiana State University, Baton Rouge, Louisiana 70803

(Received 14 March 1994)

Pore interface growth and the roughness of fracture surfaces in silica glasses have been investigated with large-scale molecular-dynamics simulations. During uniform dilation, the average pore radius R and the width W scale with the pore size s as $R \sim s^{\eta}$ and $W \sim s^{\mu}$ with $\eta = 0.48 \pm 0.03$ and $\mu = 0.50 \pm 0.03$. When the mass density is reduced to 1.4 g/cm^3, the pores grow catastrophically to cause fracture. The roughness exponent for fracture surfaces, $\alpha = 0.87 \pm 0.02$, supports experimental claims about the universality of α.

PACS numbers: 61.43.Bn, 61.20.Ja, 62.20.Mk

Porous silica has recently been the focus of many investigations [1]. This environmentally safe material has numerous technological applications [2]: It is used in thermal insulation of commercial and household refrigerators, in passive solar energy collection devices, in particle detectors, and in catalysis and chemical separation. (There is an exciting possibility of utilizing it as an embedding framework in optical switches made of quantum-confined microclusters [3].) Since these applications are due to the remarkable porous structure of the system, it is important to understand the size and spatial distributions of pores and the morphology of pore interfaces.

In recent years, a great deal of progress has been made in understanding the morphology of surfaces and interfaces. Scale-invariant surface fluctuations related to different growth processes have been observed in a wide variety of systems [4,5]: vapor deposition, fluid flow in porous media, sedimentation of granular materials, and thin-film growth. The root-mean-square surface fluctuations averaged over a distance l obey the scaling relation [4,5]

$$W \sim l^{\alpha}. \tag{1}$$

Recent experiments on a wide variety of materials reveal that fracture surfaces also exhibit scaling properties embodied in Eq. (1). Bouchaud, Lapasset, and Planès have measured the same value of α ($\approx$0.80) for four different aluminum alloys [6]. Måløy *et al.* have found that the roughness exponent of cracks in a variety of brittle materials is also close to 0.8 [7]. This led them to suggest that the roughness exponent for fracture surfaces has a universal value. Milman *et al.* [8] questioned the universality of the roughness exponent by pointing out that the measurements by Mandelbrot, Passoja, and Paullay [9] indicated a range of values for α between 0.7 and 1, implying a correlation between the roughness exponent and mechanical properties. Subsequent measurements by other groups have indicated that the value of α is around 0.8 [6]. The universality of the roughness exponent on the nanometer scale is also an unresolved issue. Milman *et al.* have suggested that the roughness exponent has different values on different length scales. Scanning tunneling microscopy data for MgO, Si, and Cu indicate that the roughness exponent is 0.6 ± 0.1 on a nanometer scale [8]. Bursill, XuDong, and JuLin [10] have found that roughness exponents for different samples of MgO, NiO, and $BaTiO_3$ lie in the range of 0.7 and 1, with an average of 0.8.

In this Letter we report large-scale molecular-dynamics (MD) calculations on amorphous silica, investigating the growth of pores with a decrease in the density of the system. We find that the average pore radius R and the width W scale with the pore size s as $R \sim s^{\eta}$ and $W \sim s^{\mu}$. For pore sizes below a density-dependent characteristic size, the exponents η and μ are 0.48 ± 0.03 and 0.50 ± 0.03, respectively; for larger pore sizes, $\eta = 0.38 \pm 0.07$ and $\mu = 0.31 \pm 0.07$. When the mass density ρ of amorphous silica is reduced to 1.4 g/cm^3, the MD simulations reveal that the system has reached the percolation threshold for fracture. Near the critical density $\rho_c = 1.4$ g/cm^3, the average size of pores grows as $|\rho - \rho_c|^{-\gamma}$ with $\gamma = 1.89 \pm 0.15$, which is close to the universal value [11]. The roughness exponent ($= 0.87 \pm 0.02$) for fracture surfaces of silica is found to be in excellent agreement with experimental measurements on different materials at mesoscopic and macroscopic length scales. These MD results tend to support the conjectured universality [6,7] of the roughness exponent even on the nanometer scale.

MD simulations for porous silica require large system sizes because structural correlations in the system span a wide range of length scales. The systems we have simulated contain up to 1.12×10^6 atoms (simulations up to 10^5 particles have been performed on the in-house Intel iPSC/860 machine and 1.12×10^6 particle simulations on IBM's 128-node SP1 system at Argonne National Laboratory). Interatomic potentials in these MD simulations include effects of charge transfer, steric repulsion, charge-dipole interaction due to electron polarizabilities of atoms, and the effect of covalent interactions through three-body

 0031-9007/94/73(17)/2336(4)$06.00 © 1994 The American Physical Society

potentials [12]. These interactions are computed with highly efficient multiresolution schemes [13–16]. The calculations have been performed on distributed-memory MIMD (multiple instructions multiple data) machines using a domain-decomposition scheme [17].

MD simulations for porous silica were performed for a wide range of mass densities from 2.2 g/cm^3 (normal density) to 1.36 g/cm^3 [18]. The normal-density glass was prepared by quenching well-thermalized molten silica at 5000 K. The molten system was cooled to 4000 K over 1000 time steps (the time step was 0.5×10^{-15} s). The system at 4000 K was thermalized for 5000 time steps. With repeated cooling and thermalization, we obtained systems at 3000, 2000, 1500, 600, and 300 K.

Figure 1 shows how well the MD results agree with neutron-scattering measurements [19,20] for the static structure factor $S_N(q)$ and the pair-correlation function $T(r)$ for the normal density silica glass at room temperature. This is by far the best agreement achieved by a MD simulation. The MD results for bond-angle distributions, photon density of states, and dynamic structure factor are also in good agreement with experimental measurements [12]. Recently MD simulations were also carried out to examine structural correlations in densified a-SiO_2 [21]. Above 40 GPa we observed a structural transformation from a corner-sharing SiO_4 tetrahedral network to a corner- and edge-sharing SiO_6 octahedral network. These results are in good agreement with high-pressure x-ray measurements by Meade, Hemley, and Mao [22].

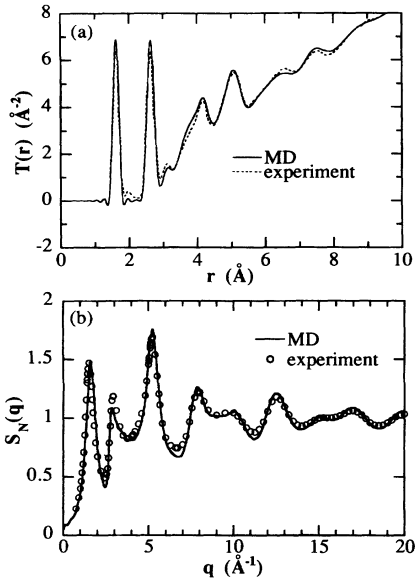

FIG. 1. (a) Neutron-scattering pair-correlation function $T(r)$ of amorphous SiO_2. Solid curve—the MD result for a 41 472 particle system; dotted curve—neutron diffraction experiment (Ref. [19]). (b) Neutron-scattering static structure factor $S_N(q)$ of amorphous SiO_2. Solid curve—the MD result for a 41 472 particle system; open circles—neutron diffraction experiment (Ref. [20]).

The low-density MD glasses were obtained by uniformly expanding the normal-density glass by a factor of 1.01–1.03 at 600 K [18,23]. Each expanded system was thermalized for 1000 steps and then brought to a local minimum-energy configuration by applying the conjugate gradient method. Atoms in these low-density glasses were assigned random velocities chosen from the Maxwell-Boltzmann distribution centered around 600 K, and then each system was thermalized for 1000 steps.

Figure 2 shows snapshots of pores in 1.12×10^6 particle systems at densities 1.8 and 1.4 g/cm^3. The pores begin to form when the density of the system is reduced to 1.8 g/cm^3. Further decrease in the density of the system causes an increase in the number of pores and also the pores coalesce to form larger entities. Pores are analyzed by dividing the MD box into smaller cubic cells (length ~4 Å) and then performing the cluster analysis of unoccupied cells using the breadth-first-search algorithm [24].

The roughness of pore interfaces is examined by calculating the width W [25],

$$W = \left\{ \frac{1}{N_s} \sum_{i=1}^{N_s} (|\mathbf{r}_i' - \mathbf{r}_0| - R)^2 \right\}^{1/2}, \qquad (2)$$

as a function of the pore volume s (the number of cells within a pore times the volume of a small cubic cell). In Eq. (2), $\{\mathbf{r}_i'\}$ denote points at the interface and $\mathbf{r}_0$ and R are the center and radius of a pore, respectively:

$$R^2 = \frac{1}{N_s} \sum_{i=1}^{N_s} |\mathbf{r}_i' - \mathbf{r}_0|^2, \qquad \mathbf{r}_0 = \frac{1}{N_v} \sum_{i=1}^{N_v} \mathbf{r}_i, \qquad (3)$$

where $\{\mathbf{r}_i\}$ denote points inside a pore.

Figure 3 shows the radius R and interface width W of pores as a function of pore volume s at a mass density of 1.44 g/cm^3. Below $\ln s = 5.3$ (corresponding to R = 46 Å), the pore radius and the interface width scale as $R \sim s^\eta$ and $W \sim s^\mu$, respectively [25], with exponents $\eta = 0.48 \pm 0.03$ and $\mu = 0.50 \pm 0.03$. Within statistical error, we find the same values of η and μ for porous silica at various densities between 1.7 and 1.4 g/cm^3. The fractal dimension of pores is $d = 1/\eta = 2.1$. Above $\ln s = 5.3$, the best fit for the MD results yields $\eta = 0.38 \pm 0.07$ and $\mu = 0.31 \pm 0.07$, and the value of the fractal dimension, $d = 2.6 \pm 0.4$, is consistent with the prediction for percolating pores [11].

Snapshots of pores in Fig. 2 reveal that there is a dramatic increase in the size of pores when the mass density is reduced to the critical value ρ_c. Near ρ_c, we find that the density dependence of the average pore size is given by

$$s_{\mathrm{av}} = \frac{\sum_s s^2 n(s)}{\sum_s s n(s)} \sim |\rho - \rho_c|^{-\gamma}, \qquad (4)$$

where $n(s)$ is the number of s clusters per site. The best fit for the MD results is obtained with $\rho_c = 1.40 \pm 0.04$ and $\gamma = 1.89 \pm 0.15$. The latter is close to the universal value (=1.8) for percolation in three dimensions [11].

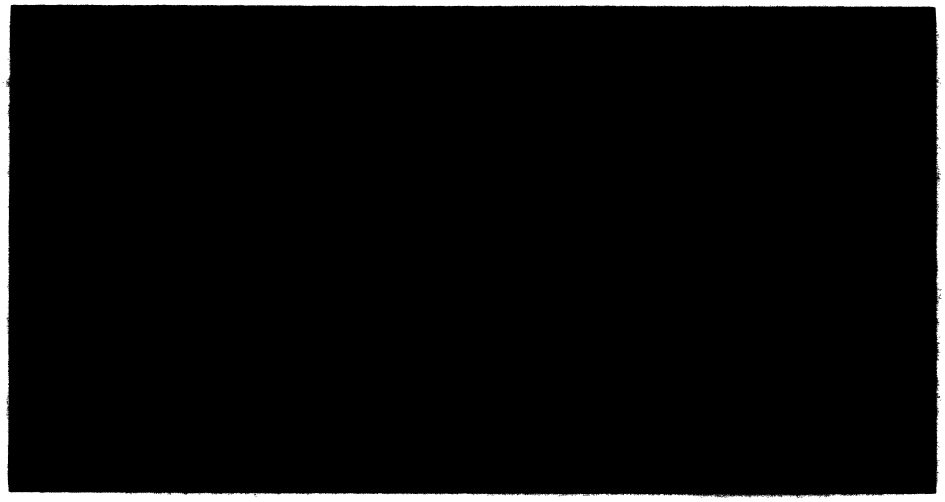

FIG. 2. Snapshots of two-dimensional slices of MD configurations of silica ($N = 1\,119\,744$) at densities 1.8 and 1.4 g/cm^3. Red and blue colors represent pores and silica, respectively.

We have also calculated the correlation length from $\xi^2 = 2\sum_s \{R(s)\}^2 s^2 n(s)/\sum_s s^2 n(s)$. Near ρ_c, $\xi \sim |\rho - \rho_c|^{-\nu}$ with $\nu = 0.9 \pm 0.2$, which is close to the universal value (= 0.9) for percolation in three dimensions [11]. For larger pores, the pore size distribution is found to scale as $n(s) \sim s^{-\tau}$ with $\tau = 2.18 \pm 0.13$ at various densities between 1.7 and 1.4 g/cm^3. The value of τ is consistent with the percolation model ($\tau = 2.2$, Ref. [11]). The range over which the scaling relation for $n(s)$ applies is identical to the range for the fractal dimension of pores, $d \sim 2.6$ (see Fig. 3).

In Fig. 4 we show one of the surfaces of the percolating pores. The roughness of this fracture surface is calculated from the height-height correlation function $g(\sigma)$ [26],

$$g(\sigma) = \left\langle [h(y + y_0, z + z_0) - h(y_0, z_0)]^2 \right\rangle^{1/2}, \quad (5)$$
$$\sigma = (y^2 + z^2)^{1/2},$$

where $h(y,z)$ is the highest vertical coordinate at the point (y,z). Figure 5 shows that the MD results for $g(\sigma)$ are well described by the relation $g(\sigma) \sim \sigma^{\alpha}$, with $\alpha = 0.87 \pm 0.02$ for $\sigma < 100$ Å. We have also calculated the structure factor $S(k) = \langle \tilde{h}(\mathbf{k})\tilde{h}(-\mathbf{k}) \rangle$, where $\tilde{h}(\mathbf{k})$ is the Fourier transform of the height fluctuation $h(y,z) - \langle h(y,z) \rangle$ [27,28]. The inset in Fig. 5 shows that $S(k)$ scales as $k^{-\delta}$, with $\delta = 3.7 \pm 0.2$. The exponents α and δ are consistent with the relation $\delta = 2\alpha + 2$ [27].

Experimental measurements on bakelite, concrete, steel, and aluminum alloys indicate that the roughness exponent α has a universal value 0.8 [7]. (Recent atomic force microscopy study of the heteroepitaxial growth

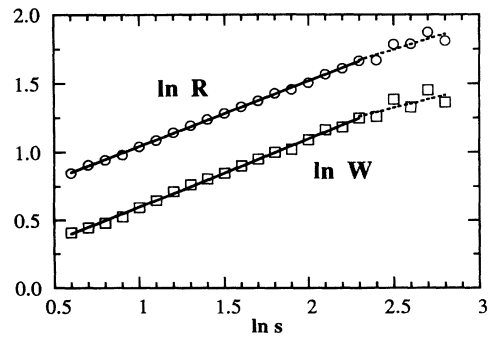

FIG. 3. Variations of the average pore radius R (open circles) and width W (open squares) with the pore size s in silica at a density of 1.44 g/cm^3. Solid and dashed curves are least squares fits below and above $\ln s = 5.3$ (corresponding to $R = 46$ Å), respectively.

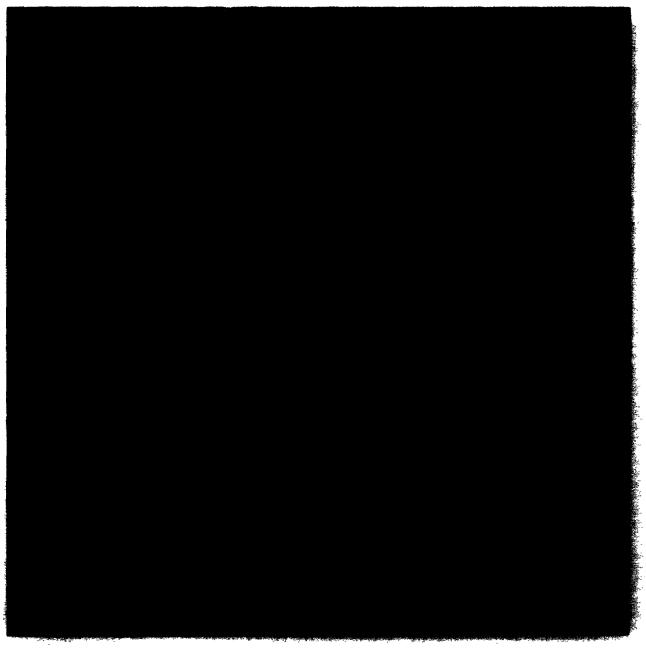

FIG. 4. Snapshot of a fracture surface resulting from a percolating pore in silica glass at a mass density of 1.4 g/cm^3. Magenta color represents the pore region.

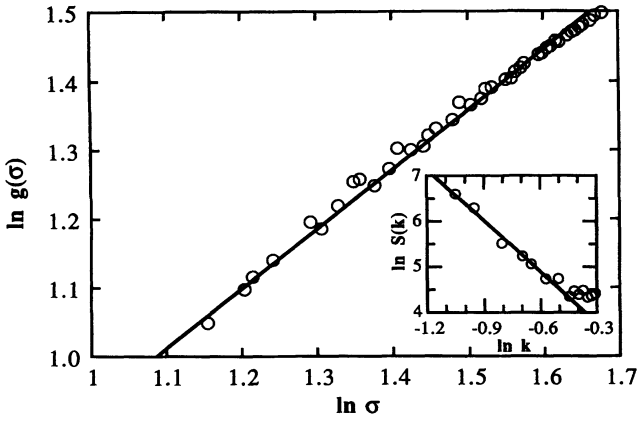

FIG. 5. Height-height correlation function (open circles) versus the in-plane distance σ for the fracture surface shown in Fig. 4. The solid curve is the best fit $g(\sigma) \sim \sigma^{\alpha}$ with $\alpha = 0.87 \pm 0.02$ for $\sigma < 100$ Å. The inset shows the structure factor $S(k)$ (open circles) and the best fit (solid curve) $S(k) \sim k^{-\delta}$ with $\delta = 3.7 \pm 0.1$.

of CuCl on CaF_2 [29] and simulations of random fuse models [30] and a two-dimensional Lennard-Jones system [31] also obtain $\alpha = 0.8$.) The MD results for the roughness exponent agree with experimental measurements, thus lending further support to claims that the roughness exponent of fracture surfaces is a material-independent quantity. Furthermore, the MD results indicate that the universality of the roughness exponent may prevail even at length scales $\leq$10 nm.

In conclusion, large-scale MD simulations reveal that during uniform dilation of silica glasses pores are "all skin and no flesh" ($R \sim \sqrt{s}$ and $W \sim \sqrt{s}$) [32]. When the density of the system is reduced to 1.4 g/cm^3, the catastrophic growth of the largest pore causes fracture in the system. The roughness exponent of resulting fracture surfaces is close to the experimental value (0.8) for many ductile and brittle materials.

We would like to thank Dr. R. Pandey for stimulating discussions. This work was supported by the U.S. Department of Energy, Grant No. DE-FG05-92ER45477. Simulations were performed on the 128-node IBM SP1 computer at Argonne and the Intel iPSC/860 in the Concurrent Computing Laboratory for Materials Simulations (CCLMS). The facilities in the CCLMS were acquired with LEQSF Enhancement Grants.

[1] J. M. Drake and J. Klafter, Phys. Today **43**, 46 (1990).
[2] J. Fricke, J. Non-Cryst. Solids **121**, 188 (1990).
[3] G. D. Stucky and J. E. MacDougall, Science **247**, 669 (1990).
[4] F. Family and T. Vicsek, J. Phys. A **18**, L75 (1985); M. Kardar, G. Parisi, and Y. C. Zhang, Phys. Rev. Lett. **56**, 889 (1986); J. Villain, J. Phys. I (France) **1**, 19 (1991); S. Das Sarma and G. V. Gaisas, Phys. Rev. Lett. **69**, 3762 (1992).
[5] *Dynamics of Fractal Surfaces,* edited by F. Family and T. Vicsek (World Scientific, Singapore, 1991).
[6] E. Bouchaud, G. Lapasset, and J. Planès, Europhys. Lett. **13**, 73 (1990); E. Bouchaud *et al.,* Phys. Rev. B **48**, 2917 (1993); J. P. Bouchaud *et al.,* Phys. Rev. Lett. **71**, 2240 (1993).
[7] K. J. Måløy, A. Hansen, E. L. Hinrichsen, and S. Roux, Phys. Rev. Lett. **68**, 213 (1992); **71**, 205 (1993).
[8] V. Y. Milman *et al.,* Phys. Rev. Lett. **71**, 204 (1993).
[9] B. B. Mandelbrot, D. E. Passoja, and A. J. Paullay, Nature (London) **308**, 721 (1984).
[10] L. A. Bursill, F. XuDong, and P. JuLin, Philos. Mag. **64**, 443 (1991).
[11] D. Stauffer, *Introduction to Percolation Theory* (Taylor & Francis, London, 1985).
[12] P. Vashishta, R. K. Kalia, J. P. Rino, and I. Ebbsjö, Phys. Rev. B **41**, 12 197 (1990).
[13] A. Nakano, R. K. Kalia, and P. Vashishta (unpublished).
[14] W. D. Street, D. J. Tildesley, and G. Saville, Mol. Phys. **35**, 639 (1978).
[15] H.-Q. Ding, N. Karasawa, and W. A. Goddard, Chem. Phys. Lett. **196**, 6 (1992); J. Chem. Phys. **97**, 4309 (1992).
[16] L. Greengard and V. Rokhlin, J. Comput. Phys. **73**, 325 (1987).
[17] R. K. Kalia, S. W. de Leeuw, A. Nakano, D. L. Greenwell, and P. Vashishta, Comput. Phys. Commun. **74**, 316 (1993); A. Nakano, P. Vashishta, and R. K. Kalia, *ibid.* **77**, 302 (1993); R. K. Kalia *et al.,* Supercomputer **54** (X-2), 11 (1993).
[18] A. Nakano, L. Bi, R. K. Kalia, and P. Vashishta, Phys. Rev. Lett. **71**, 85 (1993); Phys. Rev. B **49**, 9441 (1994).
[19] S. Susman *et al.,* Phys. Rev. B **43**, 11 076 (1991).
[20] P. A. V. Johnson, A. C. Wright, and R. N. Sinclair, J. Non-Cryst. Solids **58**, 109 (1983).
[21] W. Jin, R. K. Kalia, P. Vashishta, and J. P. Rino, Phys. Rev. Lett. **71**, 3146 (1993).
[22] C. Meade, R. J. Hemley, and H. K. Mao, Phys. Rev. Lett. **69**, 1387 (1992).
[23] First MD simulations on porous silica were performed by J. Kieffer and C. A. Angell, J. Non-Cryst. Solids **106**, 336 (1988).
[24] B. B. Lowekamp and J. C. Schug, Comput. Phys. Commun. **76**, 281 (1993).
[25] M. Plischke and Z. Rácz, Phys. Rev. Lett. **53**, 415 (1984).
[26] G. Palasantzas and J. Krim, Phys. Rev. B **48**, 2873 (1993).
[27] M. Plischke and Z. Rácz, Phys. Rev. A **32**, 3825 (1985).
[28] Since the heights become uncorrelated at distances greater than 100 Å, we calculate $S(k)$ from Fourier transforms of height fluctuations over an area of 90 × 90 Å.
[29] W. M. Tong *et al.,* Phys. Rev. Lett. **72**, 3374 (1994).
[30] A. Hansen, E. L. Hinrichsen, and S. Roux, Phys. Rev. Lett. **66**, 2476 (1991).
[31] F. F. Abraham *et al.,* Phys. Rev. Lett. **73**, 272 (1994).
[32] B. B. Mandelbrot, *Fractals: Form, Chance, and Dimension* (Freeman, San Francisco, 1977).

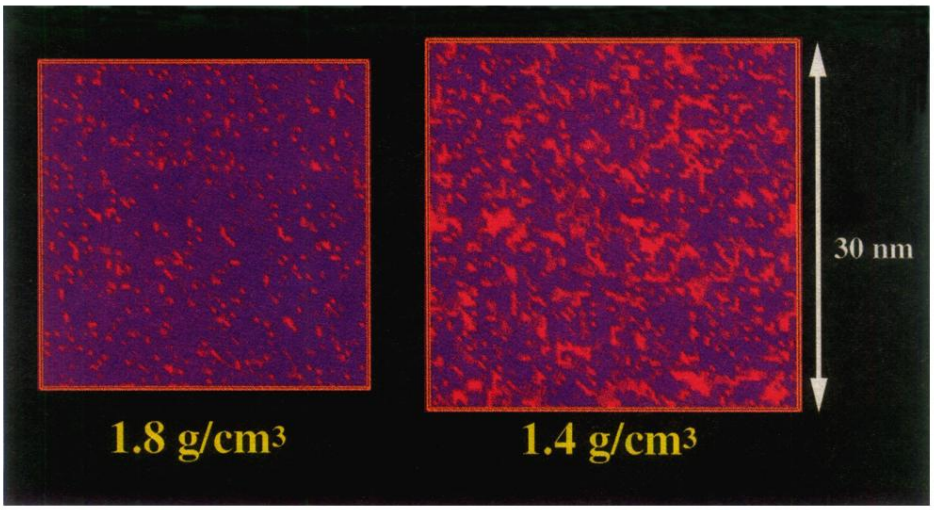

FIG. 2. Snapshots of two-dimensional slices of MD configurations of silica ($N = 1\,119\,744$) at densities 1.8 and 1.4 g/cm^3. Red and blue colors represent pores and silica, respectively.

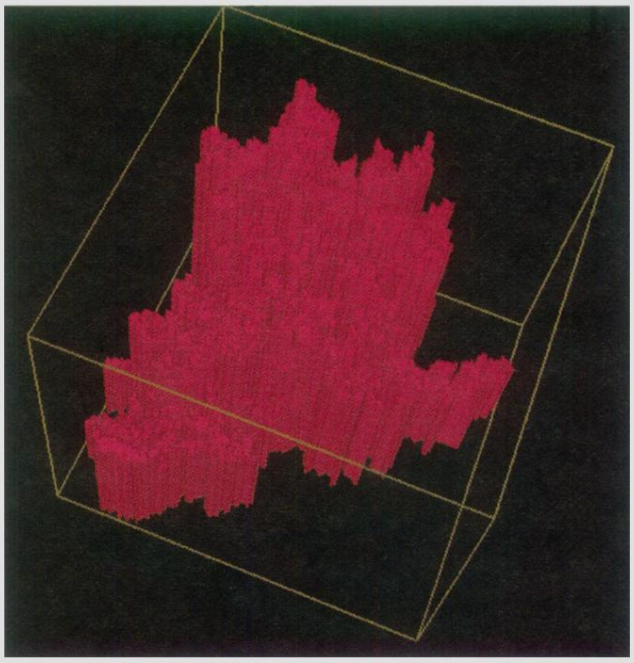

FIG. 4. Snapshot of a fracture surface resulting from a percolating pore in silica glass at a mass density of 1.4 g/cm^3. Magenta color represents the pore region.